WILEY-VCH

FULL PAPER

The Coordination Chemistry of the N-Donor Substituted Phosphazanes

Alex J. Plajer,[a]* Andrew D. Bond [a] and Dominic S. Wright [a]*

Abstract: Phosph(III)azanes, featuring the heterocyclobutane P_2N_2 ring, have now been established as building blocks in main group coordination and supramolecular compounds. Previous studies have largely involved their use as neutral P-donor ligands or as anionic N-donor ligands, derived from deprotonation of amido-phosphazanes $[RNHP(\mu\text{-}NR)]_2$. The use of neutral amido-phosphazanes themselves as chelating, H-bond donors in anion receptors has also been an area of recent interest because of the ease by which the proton acidity and anion binding constants can be modulated, by the incorporation of electron withdrawing *exo*- and *endo*-cyclic groups (R) and by the coordination of transition metals to the ring P atoms. We observed recently that the effect of P,N-chelation of metal atoms to the P atoms of *cis*-$[(2\text{-py})NHP(\mu\text{-}N^tBu)]_2$ (2-py = 2-pyridyl) not only pre-organises the N-H functionality for optimum H-bonding to anions but also results in a large increase in anion binding constants, well above those for traditional organic receptors like squaramides and ureas. Here we report a broader investigation of ligand chemistry of $[(2\text{-py})NHP(\mu\text{-}^tNBu)]_2$ (2-py = 2-pyridyl) and of the new quinolyl derivative $[(8\text{-Qu})NHP(\mu\text{-}N^tBu)]_2$ (8-Qu = 8-quinolyl). The additional N-donor functionality of the heterocyclic substituents and its position has a marked effect on the anion and metal coordination chemistry of both species, leading to novel structural behaviour and reactivity compared to unfunctionalized counterparts.

Introduction

Phosphine ligands are a central pillar of coordination chemistry and ligand design for homogenous catalysis.[1–3] Ranging from strong donor phosphines as supporting ligands for cross coupling reactions to chiral-at-phosphorus derivatives for enantioselective transformations, phosphines are omnipresent in modern chemistry.[4] However, the vast majority of these phosphines are based on organic backbones and main group counterparts based on inorganic backbones have received far less attention. In the past decade, phosphazanes, based on thermodynamically stable P-N single bonds, have emerged as excellent candidates for the construction of a range of new Lewis base donor ligand systems.[5–17] In particular, cyclo-diphosph(III)azane ligands of the type $[XP(\mu\text{-}NR)]_2$ (X = RO, R_2N, C≡CPh) (**A**, Figure 1) have been employed in the assembly of a broad range of MOF-like coordination networks and discrete macrocyclic arrangements, utilizing the P donor atoms of their P_2N_2 ring units.[18,19] Neutral phosph(III)azane ligands of this type are also of interest in catalysis. For example, late transition metal complexes of ansa-bridged dicyclophosphazanes **B** (Figure 1), in which chirality can be introduced at the diol bridge and/or at the amido R group, have allowed the observation of match and mismatch effects in enantioselective catalysis, with good enantiomeric excesses being found for the gold-catalyzed hydroamination of γ-allenyl sulfonamides and the asymmetric nickel-catalyzed three-component coupling of a diene and an aldehyde.[20] Another key area of interest has been the coordination chemistry of a range of valance-isoelectronic phosph(III)azane (**C**, Figure 1) and phosph(V)azane dianions (**D** and **E**, Figure 1), particularly in regard to the large number of donor atoms available for metal coordination and the resulting wealth of metal coordination modes observed.[7,21–25]

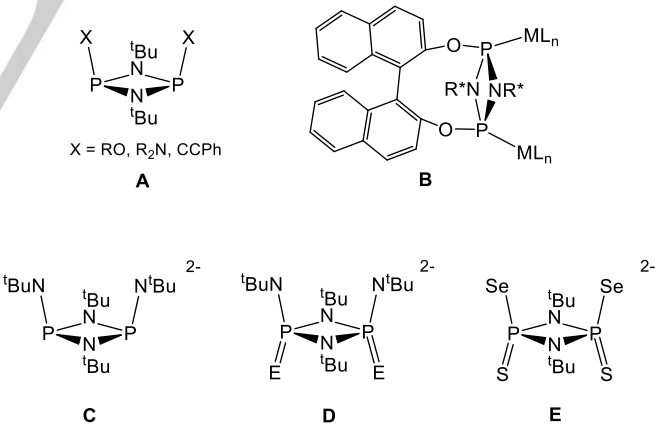

Figure 1 Neutral and dianionic phosphazane ligands studied in recent years. Neutral P-donor ligands containing exo-O, N and C groups (**A**), chiral ditopic P-donor ligands, valance-isoelectronic ligands based on phosphazane backbones (**C**, **D** and **E**).

In addition to applications as metal donor ligands, phosphazane frameworks have recently also formed the basis for a number of H-bonding anion receptor molecules. These include simple systems based on dicyclophosph(III)azanes, of the general type $[RNHP(\mu\text{-}NR)]_2$, and more elaborate phosphazane

[a] Chemistry Department, Cambridge University, Lensfield Road, Cambridge CB2 1EW (U.K.)
E-mail: dsw1000@cam.ac.uk; alex.plajer@chem.ox.ac.uk

Supporting information for this article is given via a link at the end of the document. CCDC 1997069-1997082 contain the supplementary crystallographic data for this paper. These data are provided free of charge by the joint Cambridge Crystallographic Data Centre and Fachinformationszentrum Karlsruhe Access Structures service www.ccdc.cam.ac.uk/structures.

macrocycles, like the pentamer [{P(μ-N^{t}Bu)}$_2$(NH)]$_5$.[12,13,26,27] Our recent studies of the model anion receptor [(2-py)NHP(μ-NtBu)]$_2$ (**1**), showed that the P,N-chelation of transition metals has three important effects, stabilising the P_2N_2 framework so that it becomes air- and moisture-stable, pre-organising the N-H H-bonding functionality for optimum H-bonding to anions, and dramatically increasing the polarisation of the N-H bonds (Figure 2).[28] The polarising and reorientating effects of metal coordination result in chloride affinity constants 1-2 orders of magnitude greater than established organic receptors such as ureas and squaramides.

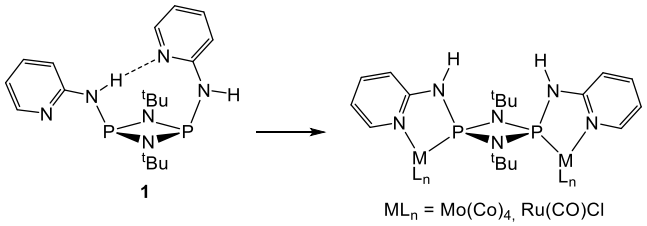

Figure 2 The reorientation effect of P,N-chelation of transition metals on the H-bond donor **1**, which also results increased polarisation of the N-H functionality.

In this paper we explore the coordination chemistry and deprotonation of [(2-py)NHP(μ-N^{t}Bu)]$_2$ (**1**) and its quinolyl relative [(8-Qu)NHP(μ-N^{t}Bu)]$_2$ (**2**) (8-Qu = 8-quinolyl). In addition, we also investigate the effects of methylation of the phosphorus atoms of **1** on its coordination behaviour and proton acidity.

Results and Discussion

Synthesis of 1 and 2

The phosphazane **1** was prepared using a modified literature procedure reported by us previously, involving condensation of the choro-phosphazane precursor [ClP(μ-N^{t}Bu)]$_2$ with (2py)NH$_2$ in the presence of Et$_3$N as a Brønsted base, which gives easy access to multi-gram quantities (in 32% yield).[28] Under the same conditions, condensation of [ClP(μ-N^{t}Bu)]$_2$ with 8-aminoquinoline yields the quinolyl-functionalised phosphazane [(8-Qu)NHP(μ-N^{t}Bu)]$_2$ (**2**) in 52% yield after crystallisation from toluene (Scheme 1, top). The room-temperature ^{31}P NMR spectrum of **2** in CDCl$_3$ shows a particularly broad singlet at δ = 102.2 ppm which results from rapid interconversion of the endo-exo and exo-exo conformers in solution. Cooling this solution results in reversion to the more thermodynamically stable exo-endo isomer, with the appearance of a second broad resonance at δ = 95.0 ppm at ca. 0°C, which sharpens at -30 °C into two 1:1 resonances (Scheme 1). This behaviour is similar to that of **1** in CDCl$_3$ for which renversion to the favoured endo-exo isomer is complete at ca. -10°C.[28] The lower activation energy for the interconversion of the exo-exo and endo-exo isomers of **2** is presumably due to the lack of transannular N-H···N$_{Ar}$ H-bonding, which is precluded by the large distance between the amido-N-H and quinolyl-N atoms (cf. **1**, in which such H-bonding does occur, see Figure 1).

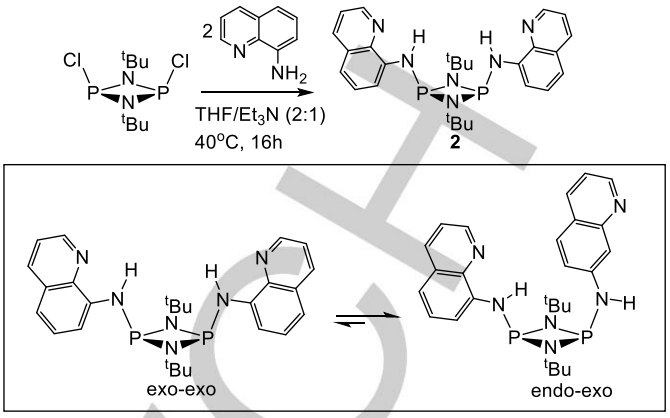

Scheme 1 Synthesis of **2** (top) and solution equilibrium between the exo-exo and endo-exo isomers.

Applications of 1 as a Ligands

We first turned our attention to exploring the coordination chemistry of **1** as a neutral ligand with transition metals. As mentioned in the introduction, we had previously shown that P,N-chelation of transition metals by **1** results in the stabilisation of the exo-exo conformation, which is the optimum arrangement for anion binding to the N-H protons.[28] In contrast, bonding to the P atoms alone, as occurs in the previously reported Au^I complex [(2-py)NHP(μ-N^{t}Bu)]$_2$(AuCl)$_2$, results in retention of the most stable endo-exo conformation of **1**.[28] A similar outcome is observed in the reaction of **1** with [(cymene)RuCl$_2$]$_2$ in the current work. However, in this case we were able to observe the effects of stepwise coordination of the two P atoms. The room-temperature reaction of **1** with 0.5 eq of [(cymene)RuCl$_2$]$_2$ in DCM gives the 1:1 complex [(2-py)NHP(μ-^{t}NBu)]$_2$[RuCl$_2$(cymene)] (**3**), as indicated in the *in situ* ^{31}P NMR spectrum, which shows 1:1 desymmetrisation of the two P environments. Layering of the reaction mixture with n-pentane gave **3** as red crystals suitable for X-ray diffraction. The solid-state structure of **3** reveals coordination of only one of the P atoms of **1** to one RuCl$_2$(cymene) fragment (Figure 3), with no further displacement of the Ru-bonded Cl-atoms by the pyridyl-N atoms of **1**. The room-temperature ^{1}H NMR spectrum of **3** in CD$_2$Cl$_2$ also indicates an asymmetrical structure, consistent with the solid-state structure, with two N-H resonances being observed at δ = 10.88 and 7.10 ppm (the former being assigned to the N-H atom that is involved in the intramolecular N-H···N$_{pyridyl}$ interaction). These resonances are shifted upfield from that seen in the uncoordinated receptor **1** (δ = 6.15 ppm in CD$_2$Cl$_2$).

Attempts to coordinate a second RuCl$_2$(cymene) fragment to **1** under similar conditions led to a mixture of **3** and the new complex [Ru$_2$Cl$_4$(cymene)][(2-py)NHP(μ-^{t}NBu)]$_2$[RuCl$_2$(cymene)] (**4**). Storage of a CD$_2$Cl$_2$ solution yielded a few single crystals of **4**, which were suitable for X-ray diffraction. The solid-state structure shows that **4** is a trinuclear ruthenium complex in which the second P bonding site of **3** coordinates a Ru$_2$Cl$_4$(cymene) fragment (Figure 3).

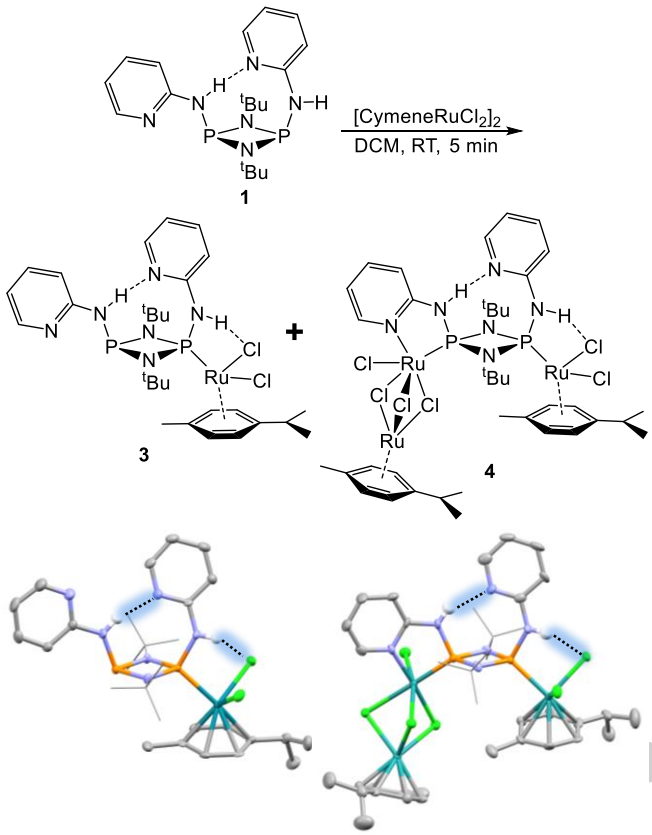

Figure 3 Top: Synthesis of **3** and **4.** Bottom: Solid-state structures of **3** and **4**. Ellipsoids shown at 40% probability; non-NH hydrogen and lattice bound solvent molecules omitted for clarity. Selected bond length [Å] and angles [°]: **3**: N_{exo}-P av. 1.68, N_{exo}-P-N_{endo} 108.5, P_{mono}-Ru 2.3435(6); **4**: N_{exo}-P av. 1.67, N_{exo}-P-N_{endo} 108.7, N_{exo}-$N_{pyridyl}$ 2.947(13), P_{mono}-Ru 2.353(3), $P_{chelate}$-Ru 2.173(3), $N_{pyridyl}$-Ru 2.054(9). Colour code: orange = P, dark green = Ru, green = Cl, blue = N, white = H, grey = C.

With the previous result in mind, we investigated how methylation of **1** could be used to block one phosphine coordination site. The previously published procedure for the methylation of [^{t}BuNHP(μ-N^{t}Bu)]$_2$ also achieves selective monomethylation of **1**.[29] Reaction of **1** with excess methyliodide in refluxing n-hexane for 16 h results in the formation of a colourless precipitate of [(2-py)NHP(μ-N^{t}Bu)P(Me)NH(2-py)]$^+$I$^-$ (**5**) (Figure 4, top). The formation of **5** is shown by the *in situ* ^{31}P NMR spectrum in $CDCl_3$ at room temperature, which shows two 1 : 1 resonances for the P(III) (δ = 97.1 ppm) and P(V) (δ = 32.2 ppm) centers, proving the quaternisation of only one of the phosphine centers of **1**.

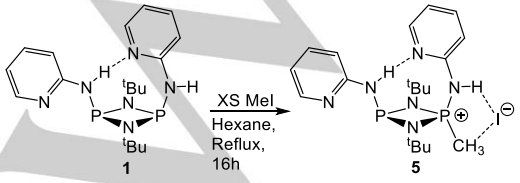

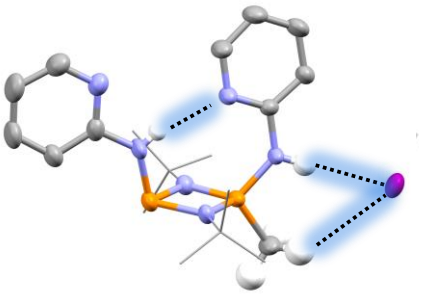

Figure 4 Top: Synthesis of **5.** Bottom: Solid-state structure of **5**. Ellipsoids shown at 40% probability; non-NH and PMe hydrogen omitted for clarity. Selected bond length [Å] and angles [°]: N_{exo}-P(Me)-N_{endo} av. 108.5, N_{exo}-P(Me)-N_{endo} av. 102.0, N_{exo}-P(Me) 1.628(4), N_{exo}-P(III) 1.666(4), N_{endo}-$N_{Pyridyl}$ 2.929(5), N_{exo}-I 3.492(4), C-I 3879(5). Colour code: orange = P, purple = I, blue = N, white = H, grey = C.

Interestingly, the iodide counter-anion of **5** is coordinated via H-bonding to one N-H and potentially the H-atoms of the P-Me$^+$ unit in the solid state structure (Figure 4, bottom). In order to confirm whether this binding geometry persists in solution, we added excess tetrabutyl- ammonium iodide to a solution of **5** in $CDCl_3$. This results in a downfield shift of the associated N-H and P-Me$^+$ resonances to a greater extent than for the other protons, and is consistent with fast-exchange binding of iodide to **5** in solution in a similar manner to that found in the solid state.

With **5** in hand we attempted coordination with a variety of transition metal precursors. Most attempts resulted in inseparable mixtures or partial decomposition of **5**, as monitored via *in situ* ^{31}P NMR spectroscopy. However, an unexpected quantitative reaction occurs between **5** and [Mo(piperidine)$_2$(CO)$_4$] (Figure 5, top).

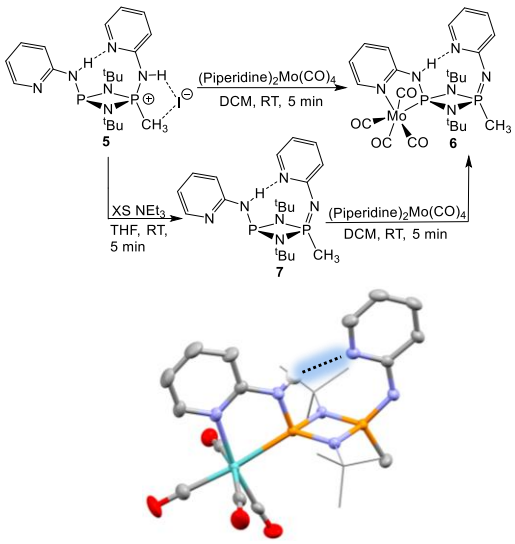

Figure 5 Top: Synthesis of **6** and **7.** Bottom: Solid-state structure of **6**. Ellipsoids shown at 40% probability; non-NH hydrogens omitted for clarity. Selected bond length [Å] and angles [°]: **6**: N_{exo}-P(Me) 1.565(2), N_{exo}-P(III) 1.680(2), $N_{Pyridyl}$-N_{exo} 3.022(3), P-Mo 2.4592(6), N-Mo 2.299(2), N-Mo-P 75.92(5), N-P(III)-N av. 104.5, N-P(V)-N av. 121.9. Colour code: orange = P, turquois = Mo, blue = N, white = H, grey = C, red = O.

The *in situ* ^{31}P NMR spectrum of the reaction mixture shows a large downfield shift of the phosphorus(III) resonance from δ = 97.1 ppm in **5** to δ = 133.1 ppm in the product. Layer diffusion of the reaction mixture with n-pentane yielded yellow crystals of [(2-py)NHP(μ-^{t}NBu)$_2$P(Me)N(2-py)]$_2$[Mo(CO)$_4$] (**6**) suitable for X-ray diffraction. The solid-state structure shows chelate coordination of the Mo(CO)$_4$ fragment by the P,N pocket of the ligand (Figure 5). However, the reaction also results in deprotonation of the P(Me)-NH(2-py) group by piperidine (a base) released in the ligand substitution reaction, resulting in a P(Me)=N(2-py) group in the framework of **6**. The *in situ* ^{1}H NMR spectrum of the reaction mixture in CDCl$_3$ confirms the formation of piperidine hydroioide. The formation of a P=N bond is apparent from the shortening of the P-N(exo) distance from 1.628(4) Å in **5** to 1.565(2) Å in **6**, while all the remaining P-N bond lengths show little or no change compared to those in **1** and **5**.

Deprotonation of **5** can also be accomplished with a base alone. Reaction of excess NEt$_3$ with **5** in DCM results in deprotonation of the phosphonium N-H proton within 5 minutes, giving [(2-py)NHP(μ-N^{t}Bu)$_2$P(Me)=N(2-py)]$_2$ (**7**) (Figure 6). The *in situ* ^{31}P NMR spectrum of the reaction mixture shows a small shift of the phosphorus(V) resonance from δ = 32.3 ppm in **5** to δ = 24.6 ppm upon deprotonation. Removal of the solvents and extraction with n-hexane to remove the Et$_3$NH$^+$I$^-$ byproduct followed by crystallisation from n-hexane yields analytically pure **7** in 75% yield.

Near quantitative formation of **6** (96% isolated yield) can also be achieved by the reaction of [Mo(piperidine)$_2$(CO)$_4$] with **7**. Reaction of **7** with [RhCOCl$_2$]$_2$ in DCM also occurs instantaneously (with CO evolution). The ^{31}P NMR of the reaction mixture confirms quantitative rhodium coordination. While the phosphorus(V) resonance remains in a similar position to that in **7** in the product of this reaction, [(2-py)NHP(μ-^{t}NBu)$_2$P(Me)N(2-py)]$_2$[Rh(CO)Cl] (**8**), a large shift in the phosphorus(III) resonance from δ = 89.3 ppm to δ = 104.4 ppm (with $^1J_{RhP}$ coupling) is observed. Layer diffusion of the concentrated reaction mixture of **7** and [RhCl(CO)$_2$]$_2$ with n-pentane yields yellow crystals of **8** (in 57% yield) suitable for X-ray diffraction. The solid-state structure confirms coordination of the [RhCOCl] fragment (Figure 6). Attempted coordination of the phosphonium salt **5** with [RhCl(CO)$_2$]$_2$ was not successful, with no CO evolution being observed.

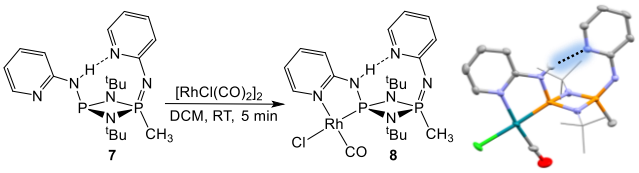

Figure 6 Left: Synthesis of **8.** Right: Solid-state structures of **8**. Ellipsoids shown at 40% probability; non-NH hydrogens omitted for clarity. Selected bond length [Å] and angles [°]: N$_{exo}$-P(Me) 1.563(4), N$_{exo}$-P(III) 1.679(2), N$_{Pyridyl}$-N$_{exo}$ 2.950(3), P-Rh 2.1525(7), N-Rh 2.118(2), N-Rh-P 82.71(6), N-P(III)-N av. 107.0, N-P(V)-N av. 122.1. Colour code: orange = P, green = Cl, dark green = Rh, blue = N, white = H, grey = C, red = O.

In contrast to **5**, which is deprotonated with weak bases such as Et$_3$N, [(2-py)NHP(μ-N^{t}Bu)]$_2$ (**1**) requires much stronger organometallic bases. Reaction of **1** with 2 equivalents of ^{n}BuLi in THF at room temperature occurs cleanly within 30 min. The *in situ* ^{31}P NMR spectrum shows a singlet resonance at δ = 120.5 ppm

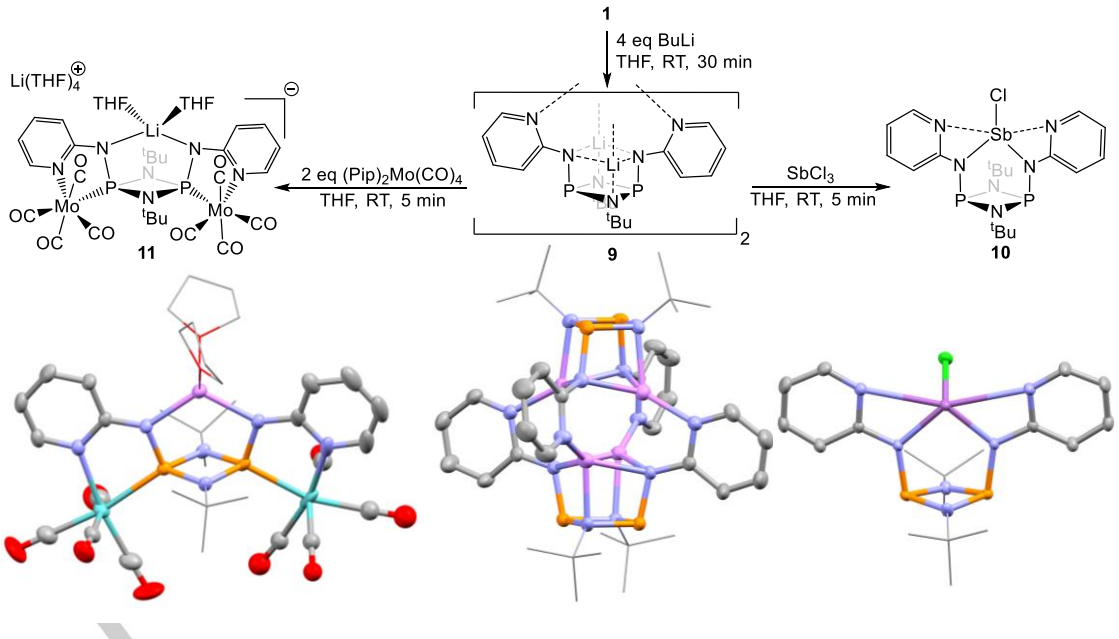

Figure 7 Top: Synthesis of **9**, **10** and **11**. Bottom: Solid-state structures of **9**, **10** and the anion of **11**. **9**: N$_{exo}$-P av. 1.69, N$_{exo}$-Li av. 2.23, N$_{endo}$-Li av. 2.21, N$_{pyridyl}$-Li av. 2.02, N$_{exo}$-Li-N$_{exo}$ av. 95.5, N$_{exo}$-Li-N$_{endo}$ av. 74.5, N$_{pyridyl}$-Li-N$_{endo}$ av. 130.5; **10**: N$_{exo}$-P av. 1.71, N-Sb av. 2.10, N$_{Pyridyl}$-Sb av. 2.73, N$_{endo}$-Sb av. 3.45. **11**: N$_{exo}$-P av. 1.65, N$_{exo}$-Li av. 2.15, N$_{Pyridyl}$-Mo av. 2.28, P-Mo av. 2.50, N$_{exo}$-Li-N$_{exo}$ 114.9(3), N$_{Pyridyl}$-Mo-P av. 73.5, N$_{exo}$-P-N$_{endo}$ av. 105.3. Colour code: orange = P, purple = Li, dark purple = Sb, green = Cl, blue = N, white = H, grey = C, red = O.

indicating the formation of the dianion $[(2\text{-py})NP(\mu\text{-}N^tBu)]_2^{2-}$ (cf. **1**, δ = 106.4ppm). Storage of the concentrated reaction mixture at -14 °C yielded crystals of the dilithiate $[\{(2\text{-py})NP(\mu\text{-}N^tBu)\}Li_2]_2$ (**9**) suitable for X-ray diffraction (Figure 7, center). In the solid-state structure, two $[\{(2\text{-py})NP(\mu\text{-}^t NBu)\}_2Li_2]$ units form a double heterocubane arrangement with D_{2d} point symmetry, in which the cubane units are connected by (pyridyl)N-Li bonds (Figure 8, middle). This arrangement is distinctly different from the previously reported lithiate of $[^tBuNHP(\mu\text{-}N^tBu)]_2$, $[\{(^tBuN)P(\mu\text{-}N^tBu)\}Li_2]_2$, which consists of a cage arrangement in which the two cubane halves interlock.[30] Interestingly, in the presence of THF this cage structure is broken up into separate cubane units in the solvate $[\{(^tBuN)P(\mu\text{-}N^tBu)\}(Li{\cdot}THF)_2]$. This behaviour is similar to **9**, in which external Lewis base solvation of the Li^+ cations is replaced by the (pyridyl)N-Li bonding of the cubane units into a single molecule.

Reaction of **9** with $SbCl_3$ (1 : 2 eq.) in THF yields $\{[(2\text{-py})NP(\mu\text{-}^t NBu)]_2SbCl\}$ (**10**) quantitatively, as seen in the *in situ* ^{31}P NMR spectrum, in which a small downfield shift of ca. 8 ppm is observed. The solid-state structure reveals tetra-coordination of a SbCl fragment by the exocyclic amido-N and pyridyl-N atoms of the $[(2\text{-py})NP(\mu\text{-}N^tBu)]_2^{2-}$ dianion (acting as an 8e donor), giving a pseudo-octahedral Sb(III) (12e) center in which one coordination site is formally occupied by a lone pair (Figure 7, right). This contrasts with the previously reported closely related complex $[\{PhNP(\mu\text{-}^t NBu)\}_2SbCl]$ in which the five coordinate Sb(III) center is bonded to the two exocyclic amido-N atoms and one of the endocyclic amido-N atoms.[31]

The lithiate **9** also reacts quantitatively with $(piperidine)_2Mo(CO)_4$ (1 : 2 eq.) in THF at room temperature, with the resulting coordination of two $Mo(CO)_4$ fragments to the $[(2\text{-py})NP(\mu\text{-}^t NBu)]_2^{2-}$ dianion (Figure 7, left). The *in situ* ^{31}P NMR spectrum shows the exclusive formation of a single product, observed as a singlet at δ = 158.8 ppm. The solid-state structure of this product, $Li(THF)_4\{[(Mo(CO)_4(2\text{-py})NP(\mu\text{-}^t NBu)]_2Li(THF)_2\}$ (**11**), (isolated in 79% yield) shows the formation of a $\{[(Mo(CO)_4(2\text{-py})NP(\mu\text{-}^t NBu)]_2Li(THF)_2\}^-$ anion which is charge balanced by a $Li(THF)_4^+$ cation (the anion is shown in Figure 8, left). The room-temperature ^7Li NMR spectrum in d_8-THF is consistent with this arrangement, with two broad singlets at δ = -1.35 and -2.65 ppm being observed (cf. a singlet δ = 3.05 ppm for **9**). It is interesting that an ion-separated arrangement is found for **11**, rather than the retention of the N_4Li_2 cubane units found in the precursor **9**. This must stem from the geometric and/or electronic constraints imposed by P,N-chelation of the $[(2\text{-py})NP(\mu\text{-}^t NBu)]_2^{2-}$ dianion to the $Mo(CO)_4$ units. Unfortunately, attempted metathesis of **10** with $SbCl_3$ or reaction with further $(piperidine)_2Mo(CO)_4$ resulted in decomposition, as monitored by *in situ* ^{31}P NMR spectroscopy.

Applications of 2 as a Ligand

Subtle differences in the reactivity and coordination chemistry result from changing the 2-py groups in $[(2\text{-py})NHP(\mu\text{-}N^tBu)]_2$ (**1**) for 8-Qu groups in $[(8\text{-Qu})NHP(\mu\text{-}N^tBu)]_2$ (**2**). A very similar outcome to reaction of **1** is observed in the reaction of **2** with $[RhCl(CO)_2]_2$ (1 : 1 eq.) in DCM, in this case resulting in near quantitative precipitation of $[(8\text{-quinolin})NHP(\mu\text{-}N^tBu)]_2(RhClCO)_2$ (**12**) (Figure 8). Complex **12** is characterised by an AA'XX' pattern with J_{RhRh} = 0 Hz at δ = 95.5 ppm in its ^{31}P NMR spectrum. However, in contrast to the previously reported complex with **1**, $[(2\text{-Py})NHP(\mu\text{-}N^tBu)]_2(RhClCO)_2$, **12**[28] is only soluble in DMSO which makes it less attractive for potential applications in membrane transport. X-ray quality crystals of **12** were obtained from a saturated 1:1 DMSO:CH_3CN mixture at 5 °C. The solid-state structure of **12** shows that the exo-exo conformation of the phosphazane unit **2** is adopted (Figure 8). This is similar to the closely related complex with **1**. There are two crystallographically distinct (chemically identical) complexes present in **12**, which show subtle differences in the binding geometry for included DMSO solvent molecules (shortest H-bonded N···O distance of 2.801(5) vs 2.920(5) Å in the two distinct complexes), illustrating that there is some flexibility in the potential anion-binding site.

The development of the N-H resonance in the ^1H NMR spectrum upon titration of **12** with TBACl in d_6-DMSO could be fitted to a 2:1 non-cooperative binding isotherm with K = (329 ± 11) M^{-1}.[32] This value can be compared to $[(2\text{-Py})NHP(\mu\text{-}N^tBu)]_2(RhClCO)_2$ with K = (1410 ± 91) M^{-1}.[28] One reason for this appears to be the lower positive polarisation of the N-H protons, which is apparent from the ^1H NMR spectrum in d_6-DMSO, i.e., δ(NH) = 9.35 ppm for $[(2\text{-Py})NHP(\mu\text{-}N^tBu)]_2(RhClCO)_2$[28] versus δ(NH) = 8.46 ppm for **12**. Interestingly, the ^1H NMR titration profile of **12** shows significant shifting of the aryl C-H resonance ($\Delta\delta$ = 0.6 ppm) closest to the chloride binding site (highlighted in sky-blue in **Error! Reference source not found.**9), which is less significant in the ^1H NMR titration profile of $[(2\text{-Py})NHP(\mu\text{-}N^tBu)]_2(RhClCO)_2$ ($\Delta\delta$ = 0.06 ppm[28]). This suggests that aryl CH···Cl^- interactions may contribute more to the overall binding interaction in **12** than in $[(2\text{-Py})NHP(\mu\text{-}N^tBu)]_2(RhClCO)_2$. These studies provide a measure of how comparatively small changes in the exocyclic amido substituent can result in dramatic changes in the binding properties of bimetallic phosphazane receptors of this type.

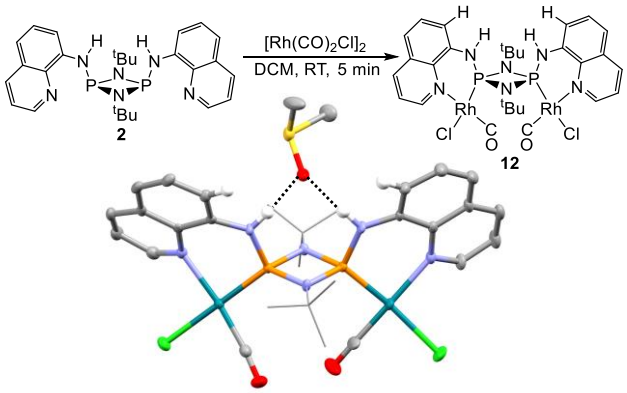

Figure 8 Top: Synthesis of **12**. Bottom: solid-state structures of **12**·DMSO. Ellipsoids shown at 40% probability; most hydrogens omitted for clarity. Selected bond length [Å] and angles [°]: N_{exo}-P av. 1.66, N_{exo}-P-N_{endo} av. 106.4, P-Rh av. 2.16, $N_{Quinolyl}$-Rh av. 2.12, $N_{Quinolyl}$-Rh-P av. 91.0.

The general coordination chemistry of **2** also differs significantly from its pyridyl analogue **1**. Oxidation of **2** with elemental selenium in THF yields $[(8\text{-Qu})NH(Se{=})P(\mu\text{-}N^tBu)]_2$ (**13**) (in 95% yield). The solid-state structure shows that **13** adopts an endo-exo conformation but with no transannular N-H•••N H-bonding supporting this arrangement (Figure 9a). The ^1H and ^{31}P NMR spectra show the presence of a single, time-averaged

species in $CDCl_3$ at room temperature, with the ^{31}P resonance splitting into two species upon cooling to -30°C (suggesting the presence of two isomers, potentially the exo-exo and endo-exo). In contrast, the ^{31}P NMR spectrum of the AuCl complex [(8-Qu)NH(ClAu)P(μ-N^{t}Bu)]$_2$ (**14**) (obtained from the reaction of **2** and 2eq (Me_2S)AuCl) consists of two broad singlet resonances at room temperature, which sharpen into a singlet and a doublet resonance upon cooling to -20 °C and merge into a singlet upon heating to 50 °C. Given that the solid-state structures of **13** (Figure 9a) and **14** (**Error! Reference source not found.**9b) show no intramolecular H-bond between the exocyclic NH proton and the opposite quinolyl group, these results show that acidification of the NH protons by AuCl also shifts the conformer equilibrium in the absence of a stabilising H-bond. This is probably due to increased repulsion of the NH dipoles upon AuCl coordination.

Reaction of **2** with 0.5 eq [(cymene)$RuCl_2$]$_2$ in $CDCl_3$ at room temperature results in coordination of one phosphine center. The solid-state structure of the product, [(8-Qu)NHP(μ-^{t}NBu)]$_2$[$RuCl_2$(cymene)] (**15**) (Figure 9c), is very similar to the previously described complex of **2** (complex **3**, Figure 4). However, in contrast to **3**, the remaining P,N-chelate coordination site of **15** does not coordinate another ruthenium fragment and no reaction between **15** and 0.5 eq [(cymene)$RuCl_2$]$_2$ was observed by *in situ* ^{31}P NMR spectroscopy. The reasons for this are unclear but probably reflect increase in ring strain resulting from the coordination of the more remote N-donor atom of the quinolyl substituent to a six-coordinate Ru center (see the structure of **4**, Figure 4). Unfortunately, attempted methylation of **2** with MeI also failed, resulting in the formation of a mixture of products.

Finally, addition of ^{n}BuLi (2 eq) to **2** in THF at room temperature gives a deep red solution (cf. a colourless solution in the case of lithation of **1**). The *in situ* ^{31}P NMR indicates that the reaction is complete after 5 min at room temperature. In contrast to the lithiate **9** (Figure 7), the isolated product of the reaction, [{(8-Qu)NP(μ-N^{t}Bu)}Li(THF)]$_2$ (**16**) (obtained in quantitative yield), does not dimerise in the solid state but forms an unsymmetrical monomeric structure, related to the previously reported solvated heterocubane [^{t}BuNP(μ-N^{t}Bu)Li(THF)]$_2$ (Figure 9d).[26] In this case, however, one Li^+ cation is tetra-coordinated by both amido-N atoms, one of the N-atoms of the P_2N_2 ring unit and a THF solvent molecule, while the other Li^+ cation is penta-coordinated by both of the two amido-N atoms, both quinolyl-N atoms and a THF solvent molecule. The ^7Li NMR spectrum of **16** shows only one resonance at 2.5 ppm at room temperature, indicating fluxional coordination of the quinolyl units to both lithium centers in solution.

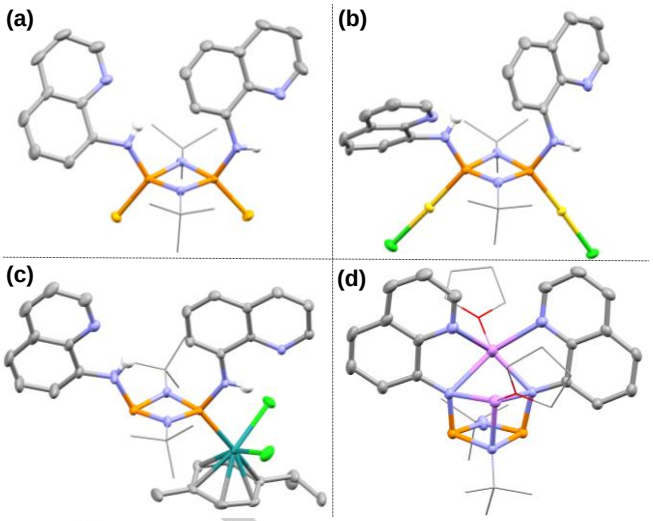

Figure 9 Solid-state structure of (a) **13**, (b) **14**, (c) **15** and (d) **16**. Displacement ellipsoids shown at 40% probability; non-NH hydrogens and lattice bound solvent molecules omitted for clarity. Selected bond length [Å] and angles [°]: (a) **13**: P-Se av. 2.08, P-N_{exo} av. 1.65, $C_{Quinolyl}$-N-P av. 131.3, N_{exo}-P-Se av. 111.2. (b) **14**: P-Au av. 2.21, P-N_{exo} av. 1.64, $C_{Quinolyl}$-N-P av. 126.7, N_{exo}-P-Au av. 111.2. (c) **15**: P-Ru 2.3379(7), P-N_{exo} av. 1.67, $C_{Quinolyl}$-N-P av. 130.5, N_{exo}-P-Ru 107.05(8). (d) **16**: $N_{Quinolyl}$-Li av. 2.28, N_{exo}-Li_{penta} av. 2.18, N_{exo}-Li_{tetra} av. 2.08, P-N_{exo} 1.68, N_{endo}-Li 2.081(4), $N_{Quinoly}$-Li-$N_{Quinolyl}$ 97.55(17), $N_{Quinoly}$-Li-N_{exo} av. 74.0, N_{exo}-Li_{penta}-N_{exo} 88.96(15), N_{exo}-Li_{tetra}-N_{exo} 94.31(16), P-N_{endo}-Li_{tetra} av. 91.9.

Conclusions

Installing donor groups in the exocylic positions in amino-cyclodiphosphazanes of the type [Ar^NNHP(μ-N^{t}Bu)]$_2$ (Ar^N = 2-py, 8-Qu) has a large effect on the coordination chemistry and reactivity of these species. The coordination of transition metal centers to one or both of the P atoms can occur, and this can be controlled by the methylation of one of the P centers. In the case of the latter, the increase in the acidity of the P(V)-bonded (2-py)NH group allows ready deprotonation and the formation of P=N bonded compounds (either concurrently with metal coordination or using a base alone). The participation of the Ar^N N-atoms in metal coordination has a significant impact on the structural chemistry compared to unfunctionalised cyclodiphosphazanes such as [^{t}BuNHP(μ-N^{t}Bu)]$_2$, as seen in complexes containing [Ar^NNP(μ-N^{t}Bu)]$_2^{2-}$ dianion ligands. The steric and electronic character of the Ar^N groups can also have a marked effect on the ability of [Ar^NNHP(μ-N^{t}Bu)]$_2$ to bind anions using the N-H functionality. Overall, our study provides key insights which will aid in the design of inorganic ligands in this area.

Experimental Section

General Experimental Methods

All experiments involving phosphorus(III)-containing species were carried out on a Schlenk line under dry nitrogen atmosphere or with the aid of a N_2-filled glove box (Saffron type α). Toluene and THF were dried under nitrogen over sodium or sodium/benzophenone, respectively, whereas

acetonitrile, chloroform and CH_2Cl_2 was dried over calcium hydride. ^1H, $^{13}C\{^1H\}$, $^{31}P\{^1H\}$ NMR spectra were recorded on a Bruker Avance 400 QNP or Bruker Avance 500 MHz cryo spectrometer. All spectra were recorded with $SiMe_4$ (^1H), H_3PO_4 (^{31}P, 85% in D_2O) as external standards and referenced to the residual solvent signal. All reagents were purchased from commercial sources and used as received without further purification unless stated differently. $[P(\mu\text{-}N^tBu)Cl]_2$ and $[P(\mu\text{-}N^tBu)NH(2\text{-}Py)]_2$ (**1**) were synthesized using the literature procedures.[12] Elemental analysis was obtained using a Perkin Elmer 240 Elemental Analyser.

Synthesis of New Compounds

Synthesis of **2**: Inside a N_2 filled glovebox, a Schlenk tube was charged with $[ClP(\mu\text{-}N^tBu)]_2$ (1.0 g, 3.6 mmol) and transferred to a Schlenk line. The solid was dissolved in 20 mL of THF and 8-aminoquinolin (1.2 g, 7.2 mmol, 2 equivalents) in 20 mL THF and 20 mL Et_3N were added dropwise at room temperature. The resulting mixture was then stirred overnight at 40 °C. The solvent was removed *in vacuo* and the resulting solid was extracted with 80 mL of n-hexane. The solvent was removed *in vacuo* until the precipitation of a faint yellow solid was observed, which was gently heated back into solution. Storage of the solution at -20 °C led to the formation of faint yellow crystals of **2** which were isolated by filtration and dried *in vacuo* (0.90 g, 1.86 mmol, 52%). ^1H NMR (25 °C, CD_3Cl, 500 MHz): δ [ppm] = 8.86 (d, 2H, $^3J_{HH}$ = 4.5 Hz, Qu), 8.10 (d, 2H, $^3J_{HH}$ = 7.0 Hz, Qu), 7.87 (bs, 2H, Qu), 7.74 (bs, 2H, Qu), 7.50 (t, 2H, $^3J_{HH}$ = 7.0 Hz, Qu), 7.40 (dd, 2H, $^3J_{HH}$ = 7.5 Hz, $^3J_{HH}$ = 6.9 Hz, Qu), 7.28 (d, 2H, $^3J_{HH}$ = 7.0 Hz, Qu), 1.23 (s, 18H, ^{t}Bu). ^{31}P NMR (25 °C, CD_3Cl, 202 MHz): δ [ppm] = 101.6 (s).

Synthesis of **3**: Inside a N_2 filled glovebox, a Schlenk tube was charged with **1** (20 mg, 0.05 mmol) and dichloro(p-cymene)ruthenium(II)dimer (16 mg, 0.025 mmol) and then transferred to a Schlenk line. 2 mL of DCM were added and the resulting red solution was stirred for 10 mins at room temperature. All volatiles were removed *in vacuo*, yielding **3** as a red solid (36mg, quantitative). X-ray quality crystals were grown by layer diffusion of a concentrated DCM solution with n-hexane. ^1H NMR (25 °C, CD_2Cl_2 , 400MHz): δ [ppm] = 10.88 (d,$^2J_{PH}$ = 4.0 Hz, 1H, NH), 8.50 (dd, $^3J_{HH}$ = 5.0 Hz, $^4J_{HH}$ = 1.7 Hz, py), 8.22 (dd, $^3J_{HH}$ = 5.0 Hz, $^4J_{HH}$ = 1.7 Hz, py), 7.58 – 7.49 (m, 2H, py), 7.11 – 6.95 (m, 2H, NH, py), 6.91 (ddd, $^3J_{HH}$ = 7.1 Hz, $^3J_{HH}$ = 5.0 Hz, $^4J_{HH}$ = 1.0 Hz, py), 6.77 (ddd, $^3J_{HH}$ = 7.1 Hz, $^3J_{HH}$ = 5.0 Hz, $^4J_{HH}$ = 1.0 Hz, py), 6.48 (d,$^2J_{PH}$ = 6.5 Hz, 1H, py), 5.65 (d,$^2J_{PH}$ = 6.0 Hz, 2H, ArH), 4.96 (d,$^2J_{PH}$ = 6.0 Hz, 2H, ArH), 3.19 (dq, $^3J_{HH}$ = 7.0 Hz, $^4J_{HH}$ = 1.5 Hz, 1H, ^{i}PrCH), 2.30 (s, 3H, Me), 1.38 (d, $^3J_{HH}$ = 7.0 Hz, 6H, ^{i}PrMe), 1.34 (s, 18H, ^{t}Bu). ^{31}P NMR (25 °C, CD_2Cl_2, 202MHz): δ [ppm] = 111.6 (d, $^2J_{PP}$ = 23.1Hz), 89.5 (d, $^2J_{PP}$ = 23.1Hz).

Synthesis of **4**: Inside a N_2 filled glovebox, a Young's NMR tube was charged with **1** (20 mg, 0.05 mmol) and dichloro(p-cymene)ruthenium(II)dimer (32 mg, 0.05 mmol) and 0.7 mL CD_2Cl_2 were added. The resulting mixture was analysed by NMR, which showed the presence of **3** and the new complex **4** (see Supporting Information Figures S6-S9). After 24 h at room temperature dark red crystals of **4** suitable for X-ray diffraction formed at the bottom of the NMR tube. The solid compound was only analysed by X-ray crystallography owing to the low isolated yield.

Synthesis of **5**: Inside a N_2 filled glovebox, a Schlenk tube was charged with **1** (1.0 g, 2.56 mmol) and then transferred to a Schlenk line. 25 mL of n-hexane and 1 mL of iodomethane (excess) were added and the resulting solution was stirred for 16 hours at 60 °C, during which a colourless precipitate of **5** formed. This was isolated by filtration, washed with 50 mL n-pentane and dried *in vacuo* (1.0 g, 1.92 mmol, 75%). X-ray quality crystals were grown by layer diffusion of a concentrated DCM solution with n-hexane. ^1H NMR (25 °C, $CDCl_3$, 400MHz): δ [ppm] = 10.42 (s, 1H, NH), 9.45 (d, $^2J_{HP}$ = 3.6Hz, 1H, NH), 8.48 (d, $^3J_{HH}$ = 4.5 Hz, 1H, py), 8.23 (d, $^3J_{HH}$ = 4.5 Hz, 1H, py), 7.91 (d, $^3J_{HH}$ = 8.2 Hz, 1H, py), 7.73 (t, $^3J_{HH}$ = 7.8 Hz, 1H, py), 7.57 (t, $^3J_{HH}$ = 7.8 Hz, 1H, py), 7.17 (t, $^3J_{HH}$ = 5.8 Hz, 1H, py), 6.92 (d, $^3J_{HH}$ = 7.9 Hz, 1H, py), 6.86 (t, $^3J_{HH}$ = 5.9 Hz, 1H, py), 2.62 (d, $^2J_{PH}$ = 15.4 Hz, 3H, PMe), 1.32 (s, 18H, ^{t}Bu). ^{31}P NMR (25°C, $CDCl_3$, 202MHz): δ [ppm] = 97.1 (d, $^2J_{PP}$= 7.0 Hz, P(III)), 32.3 (d, $^2J_{PP}$= 7.0 Hz, P(V)). Elemental analysis (%) calcd. for **5:** C 42.8, H 5.8, N 15.7; found: C 41.4, H 5.8, N 14.9.

Synthesis of **6**: Inside a N_2 filled glovebox, a Schlenk tube was charged with **7** (100 mg, 0.25 mmol) and $(piperidine)_2Mo(CO)_4$ (94 mg, 0.25 mmol, 1 eq) and then transferred to a Schlenk line. 25 mL of DCM were added and the resulting solution was stirred for 30 min at room temperature. Afterwards all volatiles were removed *in vacuo* and the resulting solid was washed with 25 mL of pentane and dried *in vacuo* yielding **6** as a yellow solid (150mg, 0.24mmol, 96%). X-ray quality crystals were grown from layer diffusion of a DCM solution with hexane. ^1H NMR (25 °C, $CDCl_3$, 400MHz): δ [ppm] = 10.08 (s, 1H, NH), 8.46 (d, $^3J_{HH}$ = 5.0 Hz, 1H, py), 8.12 (d, $^3J_{HH}$ = 5.0 Hz, 1H, py), 7.60 – 7.35 (m, 2H, py), 6.85 – 6.70 (m, 3H, py), 6.64 (t, $^3J_{HH}$ = 6.5 Hz, 1H, py), 2.05 (d, $^2J_{PH}$= 15.8 Hz, 3H, PMe), 1.42 (s, 18H, ^{t}Bu). ^{31}P NMR (25 °C, $CDCl_3$, 202MHz): δ [ppm] = 133.1 (d, $^2J_{PP}$ = 18Hz, P(III)), 22.2 (d, $^2J_{PP}$ = 18Hz, P(V)).

Synthesis of **7**: Inside a N_2 filled glovebox, a Schlenk tube was charged with **5** (532 g, 1.00 mmol) and then transferred to a Schlenk line. 25 mL of THF and 5 mL of NEt_3 (excess) were added and the resulting solution was stirred for 30 min at room temperature, during which a colourless precipitate formed. All volatiles were removed *in vacuo* and the mixture was extracted with 25mL of toluene to remove the Et_3NHI. The filtrate was collected and all volatiles were removed *in vacuo* yielding **7** as a colourless solid (400 mg, 99%). ^1H NMR (25 °C, $CDCl_3$, 400MHz): δ [ppm] = 9.92 (d, $^2J_{PH}$ = 2.5 Hz, 1H, NH), 8.29 (d, $^3J_{HH}$ = 5.0 Hz, 1H, py), 8.22 (d, $^3J_{HH}$ = 5.0 Hz, 1H, py), 7.47 (t, $^3J_{HH}$ = 7.5 Hz, 1H, py), 7.42 (t, $^3J_{HH}$ = 7.5 Hz, 1H, py), 6.85 (d, $^3J_{HH}$ = 8.0 Hz, 1H, py), 6.75 – 6.64 (m, 3H, py), 1.89 (d, $^2J_{PH}$= 16.1 Hz, 3H, PMe), 1.27 (s, 18H, ^{t}Bu).^{31}P NMR (25 °C, $CDCl_3$, 202MHz)**:** δ [ppm] = 89.3 (s, P(III)), 24.6 (s, P(V)). Elemental analysis (%) calcd. for **7**: C 56.4, H 7.5, N 20.7; found: C 56.6, H 7.5, N 20.3.

Synthesis of **8**: Inside a N_2 filled glovebox, a Schlenk tube was charged with **7** (100mg, 0.25 mmol) and $Rh_2Cl_2(CO)_4$ (50 mg, 0.13 mmol, 0.5 eq) and then transferred to a Schlenk line. 25 mL of DCM were added and the resulting solution was stirred for 30 min at room temperature. The mixture was filtered and the concentrated filtrate was layered with n-hexane. After 4 days large yellow crystals of **8** were obtained suitable for X-ray crystallography, which were isolated and dried *in vacuo* (81 mg, 0.14 mmol, 57%). ^1H NMR (25 °C, $CDCl_3$, 400MHz): δ [ppm] = 9.79 (s, 1H, NH), 9.16 (d, $^3J_{HH}$ = 5.8 Hz, 1H, py), 8.10 (d, $^3J_{HH}$ = 5.8 Hz, 1H, py), 7.69 (tt, $^3J_{HH}$ = 7.0 Hz, ^4J = 1.5 Hz, 1H, py), 7.53 (t, $^3J_{HH}$ = 7.5 Hz, 1H, py), 6.95 – 6.75 (m, 4H, py), 2.01 (d, $^2J_{PH}$= 15.8 Hz, 3H, PMe), 1.45 (s, 18H, ^{t}Bu). ^{31}P NMR (25°C, $CDCl_3$, 202MHz): δ [ppm] = 104.4 (dd, $^1J_{RhP}$ = 229 Hz, $^2J_{PP}$ = 16Hz, P(III)), 15.7 (s, P(V)).

Synthesis of **9**: Inside a N_2 filled glovebox, a Schlenk tube was charged with **1** (390 mg, 1 mmol) and then transferred to a Schlenk line. 25 mL of THF were added and 1.25 mL of ^{n}BuLi (1.6M in hexane, 2 mmol, 2 eq) were added dropwise. The resulting yellow solution was stirred at room temperature for 30 min. All volatiles were removed *in vacuo*, yielding **9** as a faint yellow solid (405 mg, quantitative). X-ray quality crystals were grown from a concentrated THF solution at -14 °C. ^1H NMR (25 °C, d_8-toluene, 400 MHz): δ [ppm] = 7.78 (d, $^3J_{HH}$ = 6.5 Hz, 2H, py), 7.57 (d, $^3J_{HH}$ = 6.5 Hz, 2H, py), 7.00 – 6.88 (m, 2H, py), 6.04 (t, $^3J_{HH}$ = 6.5 Hz, 2H, py),

1.46 (s, 18H, ^{t}Bu). ^{31}P NMR (25 °C, d_8-toluene, 202 MHz): δ [ppm] = 157.7 (s). ^{7}Li NMR (25 °C, d_8-toluene, 194 MHz): δ [ppm] = 2.95 (s).

Synthesis of **10**: Inside a N_2 filled glovebox, a Schlenk tube was charged with **1** (390 mg, 1 mmol) and then transferred to a Schlenk line. 25 mL of THF were added and 1.25 mL of ^{n}BuLi (1.6 M in hexane, 2 mmol, 2 eq) were added dropwise. The resulting yellow solution was stirred at room temperature for 30 min. A solution of $SbCl_3$ (228 mg, 1 mmol, 1 eq) in 10 mL THF was added dropwise causing the formation of a fine white precipitate. The resulting suspension was stirred for 5 min at room temperature. All volatiles were removed *in vacuo* and the solid residue was extracted with 40 mL of toluene and filtered. All volatiles were removed *in vacuo*, yielding **10** as an off-white powder (542mg, quantitative). X-ray quality crystals were grown from a saturated toluene solution at -14 °C. ^{1}H NMR (25 °C, d_8-toluene, 400 MHz): δ [ppm] = 7.97 (d, $^3J_{HH}$ = 5.2 Hz, 2H, py), 7.15 – 7.00 (m, 4H, py), 6.32 – 6.25 (m, 2H, py), 1.37 (s, 9H, ^{t}Bu), 1.12 (s, 9H, ^{t}Bu). ^{31}P NMR (25 °C, d_8-toluene, 202 MHz): δ [ppm] = 129.2 (s). Elemental analysis (%) calcd. for **10:** C 39.6, H 4.8, N 15.4; found: C 39.5, H 4.8, N 14.9.

Synthesis of **11**: Inside a N_2 filled glovebox, a Schlenk tube was charged with **9** (50 mg, 0.06 mmol) and $(piperidine)_2Mo(CO)_4$ (47 mg, 0.12 mmol, 2 eq) and then transferred to a Schlenk line. 5 mL of THF were added and the resulting solution was stirred for 10 min at room temperature, during which the colour turned orange. The reaction mixture was concentrated *in vacuo* to ca. 1.5 mL and then layered with 20 mL of n-hexane. Storage for 3 d yielded yellow crystals of **11** suitable for X-ray diffraction which were isolated and dried (62 mg, 0.05 mmol, 79%). ^{1}H NMR (25 °C, d_8-THF, 400 MHz): δ [ppm] = 8.34 (d, $^3J_{HH}$ = 7.4 Hz, 2H, py), 7.01 (t, $^3J_{HH}$ = 7.5 Hz, 2H, py), 7.43 (d, $^3J_{HH}$ = 7.5 Hz, 2H, py), 5.88 (d, $^3J_{HH}$ = 7.5 Hz, 2H, py), 3.61 (m, 24H, THF), 1.77 (m, 24H, THF), 1.50 (s, 18H, ^{t}Bu). ^{31}P NMR (25 °C, d_8-THF, 202 MHz): δ [ppm] = 158.8 (s).^{7}Li NMR (d_8-THF, 25 °C, 194 MHz): δ[ppm] = -1.35 (s), -2.65 (s).

Synthesis of **12**: Inside a N_2 filled glovebox, a Schlenk tube was charged with **2** (100 mg, 0.21 mmol) and $Rh_2(CO)_4Cl_2$ (80 mg, 0.21 mmol) and transferred to a Schlenk line. 10 mL of DCM were added and the mixture was stirred at room temperature for 30 min during which a yellow powder precipitated. The precipitate was isolated by centrifugation and dried *in vacuo* yielding **12**·DCM as a yellow powder (163 mg, 0.20 mmol, 95%).^{1}H NMR (25 °C, d_6-DMSO, 500 MHz): δ [ppm] = 9.82 (d, 2H, $^3J_{HH}$ = 6.0 Hz, Qu), 8.60 (d, 2H, $^3J_{HH}$ = 7.0 Hz, Qu), 8.46 (bs, 2H, NH), 7.72-7.58 (m, 3H, Qu), 7.47 (d, 2H, $^3J_{HH}$ = 7.0 Hz, Qu),1.60 (s, 18H, ^{t}Bu). ^{31}P NMR (25 °C, d_6-DMSO, 202 MHz): δ [ppm] = 96.3-94.6 (m). Elemental analysis (%) calcd. for **12**·DCM: C 38.3, H 3.7, N 9.2; found: C 37.9, H 3.8, N 9.0.

Synthesis of **13**: Inside a N_2 filled glovebox, a Schlenk tube was charged with **2** (200 mg, 0.40 mmol) and selenium (200 mg, excess) and transferred to a Schlenk line. 20 mL of THF were added and the mixture was stirred at room temperature. The progress of the oxidation was monitored by in situ ^{31}P NMR spectroscopy. After completion excess selenium was removed via filtration and the solvent was removed *in vacuo* yielding **13** as an air-stable white solid (265 mg, quantitative). ^{1}H NMR (25 °C, $CDCl_3$, 400 MHz): δ [ppm] = 8.83 (d, 2H, $^3J_{HH}$ = 4.7 Hz, Qu), 8.75 (bs, 2H, Qu), 8.39 (bs, 2H, NH), 8.18 (d, 2H, $^3J_{HH}$ = 6.5 Hz, Qu), 7.50 – 7.47 (m, 6H, Qu), 1.60 (s, 18H, ^{t}Bu). ^{31}P NMR (25 °C, CD_3Cl, 202 MHz): δ [ppm] = 26.7 (d accompanied by ^{77}Se satellites, $^1J_{PSe}$ = 903.9 Hz, $^2J_{PP}$ = 27.4 Hz). Elemental analysis (%) calcd. for **13**: C 48.2, H 5.0, N 13.0; found: C 47.9, H 5.0, N 12.7.

Synthesis of **14**: Inside a N_2 filled glovebox, a Schlenk tube was charged with **2** (50 mg, 0.1 mmol) and (THT)AuCl (64 mg, 0.2 mmol) (THT = tetrahydrothiophene) and transferred to a Schlenk line. 5 mL of DCM were added and the mixture was stirred at room temperature for 10 minutes. The reaction mixture was layered with 10 mL of n-pentane. Storage over 72h at room temperature yielded yellow crystals suitable for X-ray diffraction which were isolated by filtration and dried *in vacuo* yielding **14** as a crystalline solid (90 mg, 0.09 mmol, 95%). ^{1}H NMR (25 °C, $CDCl_3$, 400 MHz): δ [ppm] = 8.88 (d, $^2J_{HH}$ = 3.7 Hz, 1H, Qu), 8.49 (bs, 1H, NH), 8.29 (bs, 1H, NH), 8.24 (d, $^3J_{HH}$ = 8.3 Hz, 1H, Qu), 7.70 - 7.50 (m, 3H, Qu), 1.56 (s, 9H, ^{t}Bu). ^{31}P NMR (25 °C, $CDCl_3$, 202 MHz): δ [ppm] = 74.9 (bs), 71.0 (bs).

Synthesis of **15**: Inside a N_2 filled glovebox, a Schlenk tube was charged with **2** (50 mg, 0.1 mmol) and dichloro(cymene)ruthenium(II) dimer (32 mg, 0.05 mmol) and then transferred to a Schlenk line. 2 mL of DCM were added and the resulting red solution was stirred for 10 min at room temperature. Afterwards the reaction mixture was layered with 10 mL of pentane. Storage over 72 h at room temperature yielded red crystals suitable for X-ray diffraction which where isolated by filtration and dried *in vacuo* yielding **15**·2DCM as a crystalline solid (75 mg, 0.09 mmol, 92%). ^{1}H NMR (25 °C, $CDCl_3$, 400 MHz): δ [ppm] = 9.15 (d, $^2J_{PH}$ = 22.8 Hz, 1H, NH), 8.89 (d, $^3J_{HH}$ = 3.8 Hz, 2H, Qu), 8.61 (d, $^3J_{HH}$ = 7.9 Hz, 1H, Qu), 8.47 (d, $^3J_{HH}$ = 7.9 Hz, 1H, Qu), 8.14 (d, $^3J_{HH}$ = 7.9 Hz, 1H, Qu), 8.02 (d, $^3J_{HH}$ = 7.9 Hz, 1H, Qu), 7.80 – 7.70 (m, 2H, Qu), 7.52 – 7.38 (m, 5H, NH, Qu), 5.66 (d, $^3J_{HH}$ = 5.9 Hz, 2H, cymene), 5.13 (d, $^3J_{HH}$ = 5.9 Hz, 2H, cymene), 3.33 (quin, $^3J_{HH}$ = 7.0 Hz, 1H, cymeneCH), 2.39 (s, 3H, cymeneCH_3), 1.47 – 1.35 (m, 24H, ^{t}Bu, cymeneCH_3). ^{31}P NMR (25 °C, $CDCl_3$, 202 MHz): δ [ppm] = 97.3 (d, $^2J_{PP}$ = 26.0 Hz), 88.5 (d, $^2J_{PP}$ = 26.0 Hz). Elemental analysis (%) calcd. for **15**·2DCM**:** C 47.7, H 5.4, N 8.6; found: C 46.6, H 5.5, N 9.5.

Synthesis of **16**: Inside a N_2 filled glovebox, a Schlenk tube was charged with **2** (400 mg, 0.82 mmol) and then transferred to a Schlenk line. 20 mL of THF were added and 1.02 mL of ^{n}BuLi (1.6 M in n-hexane, 1.64 mmol, 2 eq) were added dropwise. The resulting red solution was stirred at room temperature for 30 min. All volatiles were removed *in vacuo* yielding **16** as a red solid (525 mg, quantitative). Single crystals suitable for X-ray diffraction were grown from a THF:n-hexane mixture at -14°C. ^{1}H NMR (25 °C, d_8-THF, 400 MHz): δ [ppm] = 8.04 (d, 2H, $^3J_{HH}$ = 4.0 Hz, Qu), 7.62 (d, 2H, $^3J_{HH}$ = 7.2 Hz, Qu), 7.10 (bs, 2H, Qu), 7.05 (t, 2H, $^3J_{HH}$ = 7.2 Hz, Qu), 6.55 – 6.35 (m, 4H, Qu), 1.30 (s, 18H, ^{t}Bu); ^{31}P NMR (25 °C, CD_3Cl, 202 MHz): δ [ppm] = 120.1 (s). ^{7}Li NMR (d_8-THF, 25 °C, 194 MHz): δ[ppm] = 2.50 (s).

Acknowledgements

We thank the Cambridge Trust (Vice Chancellor Scholarship for A.J.P.).

Keywords: cyclodiphosphazane • coordination chemistry • transition metals • deprotonation • X-ray crystallography

[1] R. Martin, S. L. Buchwald, *Acc. Chem. Res.* **2008**, *41*, 1461–1473.
[2] D. J. Gorin, B. D. Sherry, F. D. Toste, *Chem. Rev.* **2008**, *108*, 3351–3378.
[3] C. D. Swor, D. R. Tyler, *Coord. Chem. Rev.* **2011**, *255*, 2860–2881.
[4] K. M. Pietrusiewicz, M. Zablocka, *Chem. Rev.* **1994**, *94*, 1375–1411.
[5] M. S. Balakrishna, *Dalton Trans.* **2016**, *45*, 12252–12282.
[6] H.-C. Niu, A. J. Plajer, R. Garcia-Rodriguez, S. Singh, D. S. Wright, *Chem. – Eur. J.* **2018**, *24*, 3073–3082.
[7] A. J. Plajer, R. Garcia-Rodriguez, F. J. Rizzuto, D. S. Wright, *Chem. – Eur. J.* **2018**, *24*, 2013–2019.
[8] C. G. M. Benson, A. J. Plajer, R. García-Rodríguez, A. D. Bond, S. Singh, L. H. Gade, D. S. Wright, *Chem. Commun.* **2016**, *52*, 9683–9686.

[9] A. J. Plajer, K. Bold, F. J. Rizzuto, R. García-Rodríguez, T. K. Ronson, D. S. Wright, *Dalton Trans.* **2017**, *46*, 12775–12779.
[10] A. J. Plajer, H.-C. Niu, F. J. Rizzuto, D. S. Wright, *Dalton Trans.* **2018**, *47*, 6675–6678.
[11] A. J. Plajer, R. García-Rodríguez, C. G. M. Benson, P. D. Matthews, A. D. Bond, S. Singh, L. H. Gade, D. S. Wright, *Angew. Chem. Int. Ed.* **2017**, *56*, 9087–9090.
[12] A. J. Plajer, F. J. Rizzuto, H.-C. Niu, S. Lee, J. M. Goodman, D. S. Wright, *Angew. Chem. Int. Ed.* **2019**, *58*, 10655–10659.
[13] A. J. Plajer, J. Zhu, P. Proehm, A. D. Bond, U. F. Keyser, D. S. Wright, *J. Am. Chem. Soc.* **2019**, *141*, 8807–8815.
[14] M. Craven. D. Xiao, C. Kunstmann-Olsen, E. F. Kozhevnikova, F. Blanc, A. Steiner, I. V. Kozhevnikov, *Appl. Catal. B*., **2018**, *231*, 82-91.
[15] M. Craven, R. Yahya, E. F. Kozhevnikova, C. M. Robertson, A. Steiner, I. V. Kozhevnikov, *ChemCatChem*, **2016**, *1*, 200-208.
[16] P. Rajasekar, S. Pandey, H. Paithankar, J. Chugh, A. Steiner, R. Boomishankar, *Chem. Commun*., **2018**, *54*, 1873.
[17] T. Vijayakant, F. Ram, B. Praveenkumar, K. Shanmuganathan, R. Boomishankar, *Chem. Mater.* **2019**, *31*, 5964-5972.
[18] M. K. Pandey, H. S. Kunchur, G. S. Ananthnag, J. T. Mague, M. S. Balakrishna, *Dalton Trans.* **2019**, *48*, 3610–3624.
[19] M. M. Siddiqui, J. T. Mague, M. S. Balakrishna, *Inorg. Chem.* **2015**, *54*, 1200–1202.
[20] T. Roth, H. Wadepohl, D. S. Wright, L. H. Gade, *Chem. – Eur. J.* **2013**, *19*, 13823–13837.
[21] L. Stahl, *Coord. Chem. Rev.* **2000**, *210*, 203–250.
[22] G. R. Lief, C. J. Carrow, L. Stahl, R. J. Staples, *Organometallics* **2001**, *20*, 1629–1635.
[23] G. G. Briand, T. Chivers, M. Krahn, *Coord. Chem. Rev.* **2002**, *233–234*, 237–254.
[24] A. Nordheider, K. Hüll, J. K. D. Prentis, K. S. Athukorala Arachchige, A. M. Z. Slawin, J. D. Woollins, T. Chivers, *Inorg. Chem.* **2015**, *54*, 3043–3054.
[25] A. Nordheider, K. Hüll, K. S. A. Arachchige, A. M. Z. Slawin, J. Derek Woollins, R. Thirumoorthi, T. Chivers, *Dalton Trans.* **2015**, *44*, 5338–5346.
[26] F. F. Wolf, J.-M. Neudörfl, B. Goldfuss, *New J. Chem.* **2018**, *42*, 4854–4870.
[27] H. Klare, S. Hanft, J. M. Neudörfl, N. E. Schlörer, A. Griesbeck, B. Goldfuss, *Chem. – Eur. J.* **2014**, *20*, 11847–11855.
[28] A. J. Plajer, J. Zhu, P. Pröhm, F. J. Ruzzuto, U. F Keyzer, D. S. Wright, *J. Am. Chem. Soc.*, **2020**, *142*, 1029-1037.
[29] D. Suresh, M. S. Balakrishna, K. Rathinasamy, D. Panda, S. M. Mobin, *Dalton Trans.* **2008**, 2812–2814.
[30] J. K. Brask, T. Chivers, M. L. Krahn, M. Parvez, *Inorg. Chem.* **1999**, *38*, 290–295.
[31] D. F. Moser, I. Schranz, M. C. Gerrety, L. Stahl, R. J. Staples, *J. Chem. Soc. Dalton Trans.* **1999**, 751–758.
[32] P. Thordarson, *Chem. Soc. Rev.* **2011**, *40*, 1305–1323.

FULL PAPER

Two-Faced: phosph(III)azanes $[(Ar^N)NHP(\mu\text{-}N^tBu)]_2$ (Ar^N = 2-pyridyl, 8-quinolyl) exhibit extensive coordination chemistry and reactivity at either face of the P_2N_2 rings, coordinating soft transition metal centres with the P atoms on one face and anions or metal cations on the other, using the N or N-H groups. The additional N-donor functionality of the Ar^N groups has a large effect on the reactivity and coordination chemistry compared to unfunctionalised phosphazane counterparts.

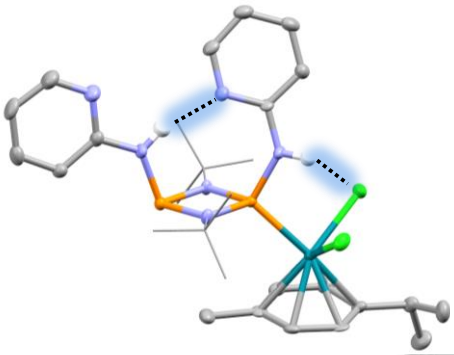

A. J. Plajer,* A. D. Bond and D. S. Wright*

Page No. – Page No.

The Coordination Chemistry of the N-Donor Substituted Phosphazanes